
HOSPITAL TRANSFER RISK PREDICTION FOR COVID-19 PATIENTS FROM A MEDICALIZED HOTEL BASED ON DIFFUSION GRAPHSAGE

A PREPRINT

 **Jun-En Ding***

Institute of Hospital and Health Care Administration
National Yang Ming Chiao Tung University
Taipei City, Taiwan
m02040013@nycu.edu.tw

 **Chih-Ho Hsu**

Far Eastern Memorial Hospital
Banqiao District, New Taipei City, Taiwan
chihhohsu.femh@gmail.com

 **Kuan-Yin Lin**

Institute of Hospital and Health Care Administration
National Yang Ming Chiao Tung University
Taipei City, Taiwan
kuanyin0828@gmail.com

 **Ling Chen**

Institute of Hospital and Health Care Administration
National Yang Ming Chiao Tung University
Taipei City, Taiwan
ling.chen@nycu.edu.tw

 **Fang-Ming Hung**

Far Eastern Memorial Hospital
Banqiao District, New Taipei City, Taiwan
philip@mail.femh.org.tw

ABSTRACT

The global COVID-19 pandemic has caused more than six million deaths worldwide. Medicalized hotels were established in Taiwan as quarantine facilities for COVID-19 patients with no or mild symptoms. Due to limited medical care available at these hotels, it is of paramount importance to identify patients at risk of clinical deterioration. This study aimed to develop and evaluate a graph-based deep learning approach for progressive hospital transfer risk prediction in a medicalized hotel setting. Vital sign measurements were obtained for 632 patients and daily patient similarity graphs were constructed. Inductive graph convolutional network models were trained on top of the temporally integrated graphs to predict hospital transfer risk. The proposed models achieved AUC scores above 0.83 for hospital transfer risk prediction based on the measurements of past 1, 2, and 3 days, outperforming baseline machine learning methods. A post-hoc analysis on the constructed diffusion-based graph using Local Clustering Coefficient discovered a high-risk cluster with significantly older mean age, higher body temperature, lower SpO₂, and shorter length of stay. Further time-to-hospital-transfer survival analysis also revealed a significant decrease in survival probability in the discovered high-risk cluster. The obtained results demonstrated promising predictability and interpretability of the proposed graph-based approach. This technique may help preemptively detect high-risk patients at community-based medical facilities similar to a medicalized hotel.

Keywords COVID-19, hospital transfer risk prediction, graph-based convolutional networks, deep learning, medicalized hotel

*Use footnote for providing further information about author (webpage, alternative address)—*not* for acknowledging funding agencies.

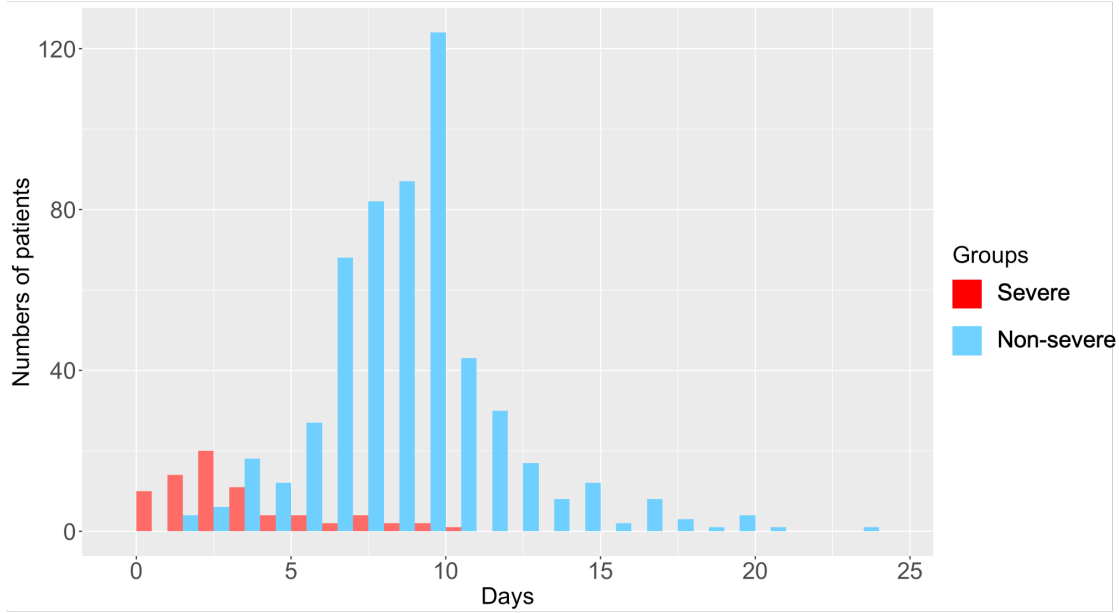


Figure 1: Daily patient count, with severe patients (being transferred on the day) colored in red and non-severe patients (remaining at the hotel on the day) in light blue. Most severe patients were transferred to a hospital within the first 3-4 days.

1 Introduction

The novel coronavirus disease 2019 (COVID-19) has become a pandemic worldwide, imposing a heavy burden on the healthcare systems. To manage the rapidly growing number of patients, temporary health care facilities, such as Fangcang shelter hospitals in China Chen et al. [2020], were established in many countries Brady et al. [2021], Spagnolello et al. [2020], Bulajic et al. [2021], Baughman et al. [2020]. In Taiwan, medicalized hotels were set up as a type of quarantine facility after a Level 3 COVID-19 alert was announced on 19 May 2021, by the Central Epidemic Command Center (CECC). Due to the limited resources and facilities in medicalized hotels, it was crucial to identify potentially severe patients early and transfer them to a hospital in time for better care. Particularly, patients experiencing rapid clinical deterioration, defined as having oxygen saturation (SpO_2) less than 94% or respiratory rate more than 30 breaths per minute, according to the COVID-19 treatment guidelines of the National Institutes of Health Kompaniyets et al. [2021], were considered as at high risk.

Machine learning (ML) is a family of algorithms that learn from data for analytic or predictive tasks James et al. [2013]. Existing COVID-19 related ML prediction models mainly focused on severity Haimovich et al. [2020a], Wu et al. [2020], Patel et al. [2020a], mortality Schwab et al. [2020], Gao et al. [2020], Hu et al. [2020], and survival time Nemati et al. [2020], Di Castelnuovo et al. [2020] predictions. In recent years, deep learning (DL), a subdomain of ML based on artificial neural networks Goodfellow et al. [2016], has shown promising performance in a wide range of applications. Deep convolutional neural networks models were introduced to diagnose COVID patients Mohamadou et al. [2020], mostly based on computed tomography (CT) scans Jangam et al. [2022], Qi et al. [2021], Lassau et al. [2021], X-rays Khan et al. [2020], P and Annavarapu [2021], and intensive care unit (ICU) data Li et al. [2020].

Graph representation is commonly used to capture objects and their relationships as nodes and edges, for example, gene-phenotype Li and Patra [2010], Wang et al. [2014] and gene-disease Wang et al. [2014] relationships. Graph Convolutional Networks (GCNs), originally evolved from Graph Neural Networks, have gained increasing attention in recent years Kipf and Welling [2016]. Several studies adapted GCNs for COVID-19 related tasks, such as COVID-19 diagnosis and severity prediction based on CT scans Keicher et al. [2021], Yu et al. [2021] or laboratory data Ferrari et al. [2022]. For example, Ferrari et al. [2022] proposed a Bayesian Structure Learning-based framework that learned a probabilistic directed acyclic graph from clinical data, such as past history and blood analysis, to identify the main causes of patient outcome. Graph representation was also used to capture social network connectivity for COVID-19 transmission based on social network data Krieg et al. [2021]. However, most existing studies relied on laboratory data or medical images Ko et al. [2020], Zhao et al. [2021], Huang et al. [2021], which were not available in medicalized hotels.

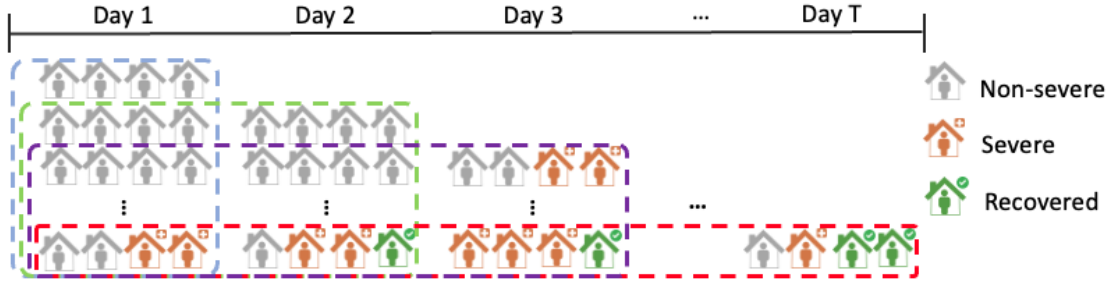


Figure 2: All patients were aligned at their arrival date. As the severe cases were transferred and non-severe cases were discharged along the time, the number of patients included in model development and testing decreased as the length of stay increased.

The current study aimed to develop and evaluate models for daily hospital transfer risk prediction based on limited patient vital signs data available at a medicalized hotel, with ML and graph-based deep learning approaches.

2 Materials and Methods

2.1 Study population and data collection protocol

In this retrospective cohort study, our dataset contained 679 patients admitted to the Banqiao medicalized hotel in New Taipei City, Taiwan, between 28 May and 7 July 2021. The hotel was managed by the Far Eastern Memorial Hospital (FEMH). During the pandemic of the alpha-variant, patients with COVID symptoms were advised to visit a hospital emergency department (ED). If tested COVID positive with stable clinical condition, the patients were transferred to a designated quarantine hotel. When arriving at the hotel, the patients were evaluated in the ambulance for triage, and 47 patients with unstable vital signs were immediately transferred to a hospital for more adequate treatment. 632 patients in total were admitted to the Banqiao medicalized hotel during the 41 days of operation. The hotel used a virtual cloud-based ward care system for medical staff to execute daily ward rounds, medical consultations, and vital signs measurements on a social media platform. Basic vital signs were measured at least once per day, eight hours apart, including body temperature (BT), pulse rate (PR), peripheral oxygen saturation (SpO₂), systolic blood pressure (SBP), and diastolic blood pressure (DBP). Throughout the quarantine period, 68 patients were transferred to a hospital due to clinical deterioration and the majority were transferred within the first 3-4 days (Fig. 1). On Day 9 of admission, afebrile and asymptomatic patients were checked for the viral load by Reverse transcription PCR (RT-PCR) from the nasal swab specimen. If the Ct (cycle threshold) value was greater than 27, the patients would be discharged the next day and asked to stay at home for another 7-day isolation. Otherwise, they would stay up to 14 days in the medicalized hotel and another 7-day isolation at home. Finally, 538 patients were discharged from the medicalized hotel. No medical staff was infected with COVID-19 during this 41-day operation Lim et al. [2021].

2.2 Data preparation

Patient data was aligned at the arrival day. We assigned a daily label to every patient based on whether they were transferred to a hospital on that day (i.e., a positive label if yes; otherwise, negative). Once a person left the medicalized hotel, either being discharged or transferred to a hospital, they were not included in the following days' modelling or testing. This design is illustrated in Fig. 2, where the number of patients involved in the study decreases as the length of stay increases.

Missing values were observed in the daily vital sign measurements with missing rates 4.93% (SpO₂), 5.48% (BT), 6.98% (PR), 81.42% (SDP), and 81.44% (DBP). To handle missing values, we used Multivariate Imputation by Chained Equations (MICE algorithm) van Buuren and Groothuis-Oudshoorn [2011], which imputed the missing values of a feature at time t based on the data before t . Due to the data imbalance issue in our dataset, we used an oversampling technique called SMOTE Wu et al. [2021] to increase the number of positive samples. The SMOTE algorithm selected a sample from the minority class and randomly selected N samples from the K nearest neighbors to synthesize M new positive samples.

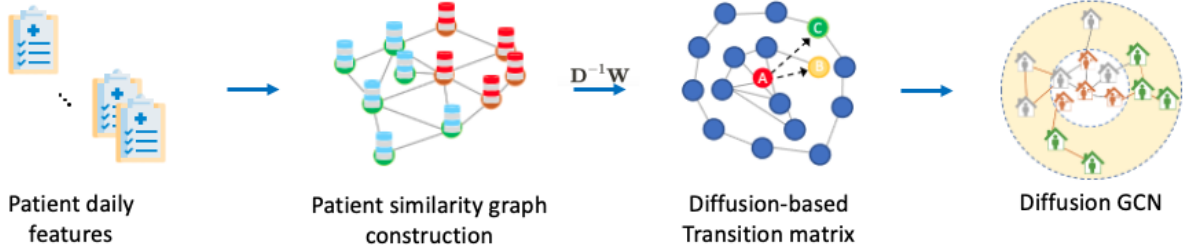


Figure 3: An overview of the proposed graph-based hospital transfer risk prediction model.

2.3 Model design

In this study, we designed a graph convolutional networks approach for hospital transfer risk prediction. As patients were aligned at their arrival, a Day T prediction refers to the use of the first T days' data to predict the hospital transfer risk on Day T . In other words, our goal was to build models capable of making predictions progressively based on the data collected so far. Unlike existing studies on COVID-19 related predictions, our models only used vital signs and explored the temporal dependencies for potential disease progression. An overview of the design can be found in Fig. 3. The main components of the proposed risk prediction framework included patient similarity graph construction and building an inductive GCN model.

2.3.1 K-neighbors graph construction

We first constructed a patient similarity graph using the k-neighbors method. Let patient features on Day t be represented as a matrix $\mathbf{X}^{(t)} \in \mathbb{R}^{n \times p}$, $t = 1, \dots, T$. Where n is the number of patients included on Day t and p is the number of vital signs measurements. To capture similarities among patients on each day, we built a temporal weighted adjacency matrix using K-neighbors for the day. In a K-neighborhood, two data points i and j connected by an edge (i, j) if i is amongst the K nearest neighbors of j or vice versa. A weighted graph is defined as $\mathcal{G}(V, E, \mathbf{W})$, where V and E are the sets of nodes and edges respectively, and \mathbf{W} is a weighted matrix computed from a function of Gaussian kernel defined as below:

$$W_{ij} = W(X_i, X_j) = \begin{cases} \exp(-\frac{\|X_i - X_j\|^2}{\alpha}), & \text{if } X_i \in \mathcal{N}(X_j) \text{ or } X_j \in \mathcal{N}(X_i) \\ 0, & \text{if } X_i \notin \mathcal{N}(X_j) \text{ or } X_j \notin \mathcal{N}(X_i) \end{cases}$$

where W_{ij} is an undirected edge of vertices i and j , X_i denotes row i in \mathbf{X} , and α is a scale parameter.

2.3.2 Diffusion graph construction

We further extended the k-neighbors-based graph to a diffusion-based graph to capture disease progression over time. A transition matrix can be defined as $\mathbf{D}^{-1}\mathbf{W}$ where the degree matrix is defined as $\mathbf{D} = \text{diag}(d_{11}, d_{22}, \dots, d_{nn})$, where d_{ii} is the sum of row i in W_{ij} . To build a diffusion transition graph, given the transition matrices of the weighted graphs $[\mathcal{G}^{(1)}, \dots, \mathcal{G}^{(t)}, \dots, \mathcal{G}^{(T)}]$ defined previously for Day 1, ..., Day T , the diffusion distances Lim et al. [2021] on the graph can be computed as the linear combination of weighted graph of infinite random walk and stationary diffusion distribution \mathcal{P} Li et al. [2018]:

$$\mathcal{P} = \sum_{t=1}^{\infty} (\mathbf{D}^{-1}\mathbf{W})^t$$

Therefore, we can use the patient features up to Day T as a T -step truncation process in a finite diffusion step. Alternatively, the \mathcal{P} can be interpreted as the cumulative probability of the patient's state in a diffusion process on Day T .

2.3.3 Inductive GCNs

Graph convolutional networks (GCNs) Kipf and Welling [2016] is a deep learning architecture commonly applied to graph node classification problems. Traditional graph convolutional networks belong to a transductive learning approach, where both training and testing data are used to construct the learning graph at the training time. However, a transductive approach is not practical in most medical settings, since new patient data is often unavailable at the model development time. To tackle this problem, we adapted a graph convolutional network called GraphSAGE Hamilton et al. [2017] capable of inductively predicting the unseen nodes. Using a sampling strategy, the model was able to learn node embeddings based on neighboring node features rather than the entire graph. When an inference was performed, the learned information can be aggregated to the weight of the target node. Given a patient similarity graph constructed previously with the set of nodes $V = \{v_1, \dots, v_n\}$, the model computed for every node its connectivity with its depth k for $k = 1, \dots, K$, using K network layers. Let $\mathcal{N}(v)$ denote the neighborhood of v and $h_{\mathcal{N}(v)}^{k-1}$ be the aggregated representation of v 's immediate neighborhood $\{h_u^{k-1}, \forall u \in \mathcal{N}(v)\}$ at depth $k - 1$. Then the convolutional propagation at layer k for node v is defined based on the concatenation of its previous layer output and its current aggregated neighborhood:

$$h_v^k = \sigma(W^k \cdot \text{CONCAT}(h_v^{k-1}, h_{\mathcal{N}(v)}^k))$$

Let z_v be the output of the final aggregated information from h_v^k , $\forall v \in \mathcal{V}$. To train an empirical graph model end-to-end, we used a graph-based cross-entropy loss function.

$$\mathcal{L}_G = - \sum_{l \in \mathcal{Y}_L} y_l^T \ln(\text{softmax}(z_v^{(L)}))$$

where \mathcal{Y}_L is the set of labeled nodes, and y_l the ground truth represented by the one-hot encoding.

2.4 Statistical analysis

Continuous variables were expressed as mean \pm SD or median (range) for normally and non-normally distributed data, respectively. To assess normal distribution, the Kolmogorov-Smirnov test was performed. Continuous variables were compared using Student t-test or Wilcoxon rank sum test, and categorical variables were compared using Pearson's Chi-squared or Fisher's exact test as appropriate. A p -value < 0.05 was considered statistically significant.

The performance of the transfer risk classification was analyzed by sensitivity (SEC), specificity (SPE), the receiver operating characteristic curve (ROC), and measured by the area under the ROC curve (AUC). Local Clustering Coefficient (LCC) was used to measure node connectivity in graph. All statistical analysis was performed using RStudio IDE tools (<https://www.rstudio.com/>) or Python SciPy package (www.scipy.org).

2.5 Experimental settings

The entire study cohort was partitioned into a training set (60%) and a testing set (40%) using stratified random sampling. The choice of 60/40 partitioning, instead of the conventional 80/20 or 70/30, was based on the limited number of positive cases ($< 12\%$) in our dataset. Baseline ML methods compared included Linear Discriminant Analysis (LDA), Support Vector Machine (SVM), Random Forest (RF), K-nearest neighbors (KNN) and Logistic regression (LR). The features of different days were concatenated for the ML based models. Since the original GraphSAGE model relied on data naturally containing linkages between objects, e.g., social networks and protein interactions, it was not directly comparable on our patient data. Therefore, we designed three versions of GraphSAGE-based GCN models for the evaluation as follows.

- KNN-GCN: It used K-neighbors method to find K nearest neighbors for every given node and to construct a daily patient similarity graph. For a Day T prediction, the final graph was obtained by aggregating graphs of Day 1, 2, ..., T , based on which a GCN was trained for classification.
- Diffusion-GCN: It used an additional diffusion process to aggregate daily patient similarity graphs, based on which a GCN was trained for classification.
- Diffusion-GCN (+age): It used Diffusion-GCN with age as an additional feature, included as node attribute for training.

The number of clusters K for the K-neighbors method used to build the adjacency graphs in our approach was experimentally set to $K=200$ for the training set and $K=100$ for the validation set, due to limited data size in the validation set. For the settings of GCNs, the mean aggregator was used as the aggregator, the number of hidden layers was set to 2, and each layer size was 62. Unlike traditional GCN methods, we subsampled 50 random nodes from the neighborhood for each hidden layer for training. To prevent overfitting, the dropout rate was set to 0.1. The network was trained using an Adam optimizer with a learning rate of 0.05 and an early stopping strategy.

2.6 Data availability

The dataset generated during and/or analysed during the current study is not publicly available due to ethical and data safety reasons but is available from the corresponding author on reasonable request.

Table 1: Summary statistics of the study population

Covariate	Non-severe (N=558) ¹	Severe (N=74) ¹	p -value ²
Age	40 (19) [39, 42]	51 (20) [46, 56]	<0.001
Gender			0.6
Female	273 (49) [45, 53]	34 (46) [34, 58]	
Male	285 (51) [47, 55]	40 (54) [42, 46]	
Vital signs³			
Body Temperature (°C)	36 (0.63) [36, 36]	37 (0.50) [36, 37]	<0.001
SpO ₂ (%)	96 (1.11) [96, 96]	95 (1.91) [95, 95]	<0.001
Pulse rate (bpm)	88 (11) [87, 89]	93 (11) [91, 96]	<0.001
Systolic blood pressure (mm Hg)	85 (16) [84, 86]	81 (10) [78, 83]	0.1
Diastolic blood pressure (mm Hg)	126 (14) [125, 127]	127 (13) [124, 130]	0.8
Comorbidities			
Diabetes	26 (4.7) [3.1, 6.8]	11 (15.0) [8.0, 25.0]	0.002
Cardiovascular	14 (2.5) [1.4, 4.3]	5 (6.8) [2.5, 16.0]	0.06
Obesity	19 (3.4) [2.1, 5.4]	4 (5.4) [1.7, 14.0]	0.3
COPD ⁴	48 (8.6) [6.5, 11.0]	8 (11.0) [5.1, 21.0]	0.5
Length of stay (day)	9 (3.0) [9.0, 9.5]	3 (2.0) [2.2, 3.4]	<0.001

¹ n (%); Mean (SD); 95% Confidence Interval [lower limit, upper limit]

² Pearson’s Chi-squared test; Wilcoxon rank sum test; Fisher’s exact test.

³ Computed based on the first three days of data.

⁴ COPD: Chronic Obstructive Pulmonary Disease.

A total of 632 patients were included in this retrospective study, with a mean age of 41 ± 19 years old. Table 1 summarized the descriptive statistics of patient demographics, vital signs, and comorbidities. The mean age of the severe group was significantly higher than the non-severe group (51 vs. 40, $p < 0.001$), and so was length of stay (3 vs. 9, $p < 0.001$). Amongst five comorbidities, diabetes mellitus prevalence was significant between the two groups (11 vs. 26, $p < 0.002$). Between the severe and non-severe groups, the differences were statistically significant for body temperature, SpO₂, and pulse rate ($p < 0.001$).

2.7 Severity classification and model validation

We evaluated the proposed GCN models for daily transfer risk classification against five popular ML methods. Table 2 compares model performances in terms of AUC, sensitivity, and specificity. Amongst ML methods, all except Random Forest suffered from zero sensitivity at some stage, which indicated that the models were totally biased towards the negative class. Random Forest was comparable to KNN-GCN and Diffusion-GCN(+age) on Day 1 prediction. However, starting from Day 2, GCN models overtook Random Forest, especially in AUC and sensitivity, achieving AUCs ≥ 0.83 for Day 1, 2, and 3 predictions.

Amongst GCN models, KNN-GCN and Diffusion-GCN were comparable. While KNN-GCN outperformed Diffusion-GCN on Day 1 and Day 2, especially in sensitivity (≥ 0.67), Diffusion-GCN overtook KNN-GCN on Day 3 in both AUC (0.94) and sensitivity (0.75). Therefore, Diffusion-GCN demonstrated more stable performance for predictions

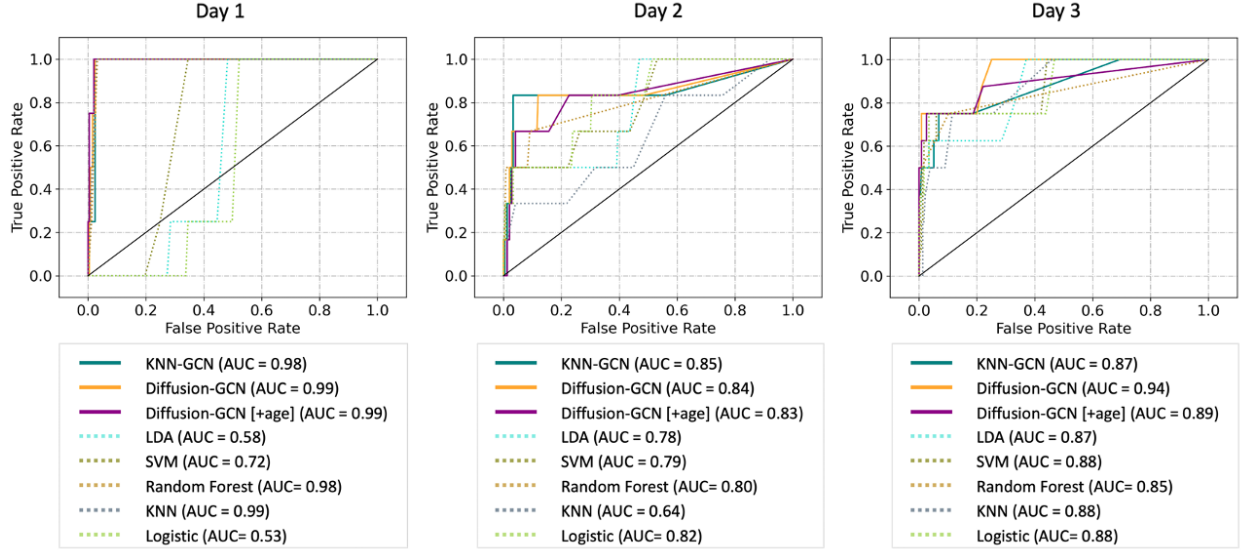


Figure 4: ROC curves of models predictions on Day 1, 2 and 3 on the testing dataset

based on more days of data. This can be explained by the ability of a diffusion process to aggregate progression over time. ROC curves in Fig. 4 also demonstrated that the proposed GCN models outperformed baseline ML methods.

2.8 Post-hoc graph analysis

To further analyze the constructed diffusion-based graphs visually, we filtered out weights smaller than 0.014 for the graph on Day 3 and plotted a fully connected graph, with severe cases marked red and non-severe cases light blue based on the ground truth. As shown in Fig. 5 (A), a cluster of red points appears to be more concentrated.

Based on the observation, we used Local Clustering Coefficient (LCC) Ferraz de Arruda et al. [2018] to analyze the degree of aggregation between nodes on the graph to find concentrated clusters. The histogram of the resulting LCC coefficients was plotted in Fig. 5 (B), with the severe group marked in red and non-severe group in light blue. In general, the higher the LCC coefficient, the higher the degree of interconnection between the nodes. With a cutoff of $LCC=0.75$, we were able to identify a densely connected cluster of severe cases on the graph, as shown in the red circle in Fig. 5 (C). Comparing the summary statistics of identified high-risk cluster and the remaining cluster, Table 3 shows that the patients in the high-risk cluster were significantly older (54 vs. 41 years old, $p=0.003$), with significantly

Table 2: Model performances on Day 1, 2, and 3 predictions on the testing dataset

	Day 1			Day 2			Day 3		
	AUC	SEN	SPE	AUC	SEN	SPE	AUC	SEN	SPE
KNN-GCN	0.98	1.00	0.98	0.85	0.67	0.97	0.87	0.63	0.94
Diffusion-GCN	0.99	0.75	0.98	0.84	0.50	0.97	0.94	0.75	0.91
Diffusion-GCN (+age)	0.99	1.00	0.98	0.83	0.33	0.97	0.89	0.75	0.93
LDA	0.58	0.00	0.98	0.78	0.33	0.98	0.87	0.63	0.96
SVM	0.72	0.00	0.99	0.79	0.17	0.99	0.88	0.63	0.96
RF	0.98	1.00	0.97	0.80	0.50	0.99	0.85	0.50	0.99
KNN	0.99	1.00	0.92	0.64	0.00	1.00	0.88	0.00	1.00
LR	0.53	0.00	0.99	0.82	0.33	0.97	0.88	0.50	0.97

GCN: Graph Convolutional Networks; LDA: Linear Discriminant Analysis; SVM: Support Vector Machine; RF: Random Forest; KNN: K-nearest neighbors; LR: Logistic Regression; AUC: area under the ROC curve; SEN: Sensitivity; SPE: Specificity.

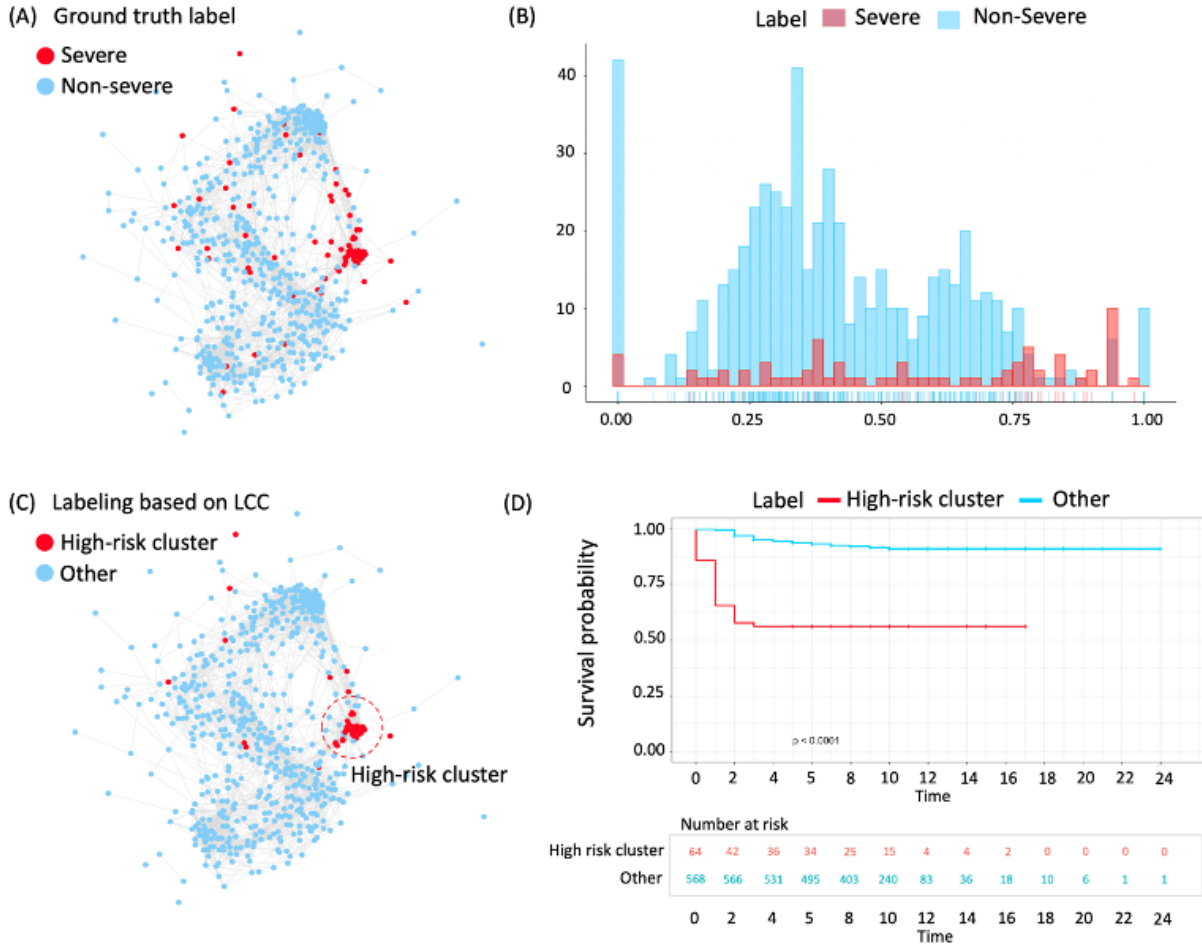


Figure 5: (A) Constructed diffusion-based patient similarity graph, with nodes colored according to the ground truth labels. (B) An LCC histogram calculated based on the graph. (C) Using the LCC cut-point to color the graph. (D) Time-to-hospital-transfer survival analysis on the discovered clusters.

higher BT (36.57 vs. 36.21, $p < 0.001$), lower SpO₂ (95.10 vs. 96.03, $p < 0.05$), and shorter length of stay (1 vs. 9 days, $p < 0.001$). Additionally, the LCC of the high-risk cluster was significantly higher (0.86 vs. 0.41, $p < 0.001$).

We also conducted survival analysis using the cox survival model for the clusters. Fig. 5 (D) shows the Kaplan-Meier curves for the clusters. The identified high-risk severe cluster (red) had the highest risk, with the time-to-hospital-transfer survival probability lower than 60% in two days. For the remaining cluster (green), the survival probabilities showed a relatively stable step probability function decreasing over time.

3 Discussion

During the outbreak of a massive infectious disease, an accurate and easily-available risk stratification system was necessary to find potential critically ill patients and assign scarce medical resources to those in need Patel et al. [2020b], Bolourani et al. [2020], Kim et al. [2020]. According to COVID-19 treatment guidelines from WHO Kompaniyets et al. [2021], remdesivir and dexamethasone were recommended to prevent disease progression for patients needing hospitalization and oxygen supplement. However, the timing of giving remdesivir is important Siemieniuk et al. [2020]. Therefore, a timely and accurate predictive system may help identify patients in need.

In this study, we developed and evaluated a graph-based deep learning approach to distinguishing severe COVID-19 patients who needed to be transferred to a hospital for further medical and respiratory support. Overall, the proposed GCN models outperformed all the ML models compared, demonstrating their superior abilities to differentiate between

Table 3: Summary statistics of LCC-discovered clusters

	High-risk (N=28) ¹	Other (N=604) ¹	p-value ²
Age	54 (21)	41 (19)	0.003
Gender			0.113
Female	9 (32)	298 (49)	
Male	19 (68)	306 (51)	
Vital signs			
Body Temperature (BT) (°C)	36.57 (0.49)	36.21 (0.63)	<0.001
SpO ₂ (%)	95.10 (2.40)	96.03 (1.20)	0.049
Pulse rate (bpm)	91 (8)	89 (11)	0.12
Systolic blood pressure (mm Hg)	83 (8)	84 (16)	0.4
Diastolic blood pressure (mm Hg)	127 (11)	126 (14)	0.6
Local clustering coefficient	0.86 (0.07)	0.41 (0.22)	<0.001
Length of stay (day)	1 (1)	9 (3)	<0.001

¹ Mean (SD); n (%).

² Wilcoxon rank sum test; Pearson’s Chi-squared test.

severe and non-severe cases using a graph representation (all AUCs ≥ 0.83). Although the proposed KNN-GCN and Diffusion-GCN were comparable, Diffusion-GCN demonstrated more stable performance for predictions based on more days of data.

Identifying high-risk COVID-19 patients was important to allocate limited medical resources during an outbreak. CURB-65 Lim et al. [2003] and qSOFA Seymour et al. [2016] were commonly used predictive tools for estimating mortality for community-acquired pneumonia and suspected sepsis respectively. Haimovich et al developed COVID-19 severity index (CSI) using XGBoost algorithm and quick COVID-severity index (qCSI) using logistic regression, based on respiratory rate, pulse oximetry, and oxygen flow rate Haimovich et al. [2020b]. The reported AUCs for CSI (76%) and qCSI (81%) outperformed classic CURB65 (50%) and qSOFA (59%) based on a dataset of 1792 patients who might develop respiratory failure in the emergent department. However, unlike our progressive prediction approach, their model predicted at the 4 hour mark after admission and did not consider disease progression over time.

The findings in our study echoed existing medical research. Our data showed that most severe patients became progressively ill within 3-4 days of their stay, which corresponded to the mean time from symptom onset to hospitalization reported in the study by Pellis et al (2.62 days in Singapore, 4.41 days in Hong Kong, and 5.14 days in the UK) Pellis et al. [2021]. A large cross-sectional study by Kompaniyets et al based on more than 540,000 adults hospitalized with COVID-19 Kompaniyets et al. [2021] found that the death risk ratio increased from 3.4 to 18.5 when the patients’ age group changed from 40-49 to 50-64. Our study also discovered a high-risk cluster that had significantly older mean age (54.2 vs. 40.9, $p < 0.01$).

As the recent prevalent SARS-CoV-2 omicron strain caused less severe outcomes than previously dominant variants, public health policies for COVID-19 management started to encourage community-based health care rather than hospital-based treatment. However, unlike our work, most existing studies relied on the radiologic and laboratory data, which was not accessible in a community-based health care center, like the medicalized hotel in this study.

Furthermore, our study demonstrated the feasibility of continuous remote patient monitoring echoing the studies of Downey et al. [2018], Larimer et al. [2021], as the data used in this study was collected via a virtual cloud-based ward care system, which was an extension from current hospital information system and could be easily implemented. The limitation of the current study lies in that the majority of the severe patients were transferred to a hospital within the first three days; therefore, there was not enough positive cases for training robust models for predictions over a longer period, which a larger dataset in the future may help.

4 Conclusion

Identifying potentially severe COVID-19 patients who needed to be transferred from a medicalized hotel to a hospital is critical for timely medical and respiratory support. In this study, we developed and evaluated a graph-based progressive hospital transfer risk prediction approach based on daily progression of vital signs and accumulated transition probability. Although this study was based on patient data when the alpha-variant was the dominant COVID-19 strain, our approach demonstrated superior performance and potential applicability to future prediction tasks with limited longitudinal measurements at hand, as in the case of a medicalized hotel.

References

- Simiao Chen, Zongjiu Zhang, Juntao Yang, Jian Wang, Xiaohui Zhai, Till Bärnighausen, and Chen Wang. Fangcang shelter hospitals: a novel concept for responding to public health emergencies. *Lancet (London, England)*, 395(10232):1305–1314, 2020. ISSN 0140-6736. doi:[https://doi.org/10.1016/s0140-6736\(20\)30744-3](https://doi.org/10.1016/s0140-6736(20)30744-3).
- Kevin Brady, Dave Milzman, Edward Walton, Darren Sommer, Alan Neustadt, and Anthony Napoli. Uniformed Services and the Field Hospital Experience During Coronavirus Disease 2019 (SARS-CoV-2) Pandemic: Open to Closure in 30 Days With 1,100 Patients: The Javits New York Medical Station. *Military Medicine*, pages usab003–, 2021. ISSN 1930-613X. doi:<https://doi.org/10.1093/milmed/usab003>.
- Ornella Spagnolello, Silvia Rota, Oliviero Francesco Valoti, Claudio Cozzini, Pietro Parrino, Gina Portella, and Martin Langer. Bergamo Field Hospital Confronting COVID-19: Operating Instructions. *Disaster Medicine and Public Health Preparedness*, pages 1–3, 2020. ISSN 1935-7893. doi:<https://doi.org/10.1017/dmp.2020.447>.
- Bojana Bulajic, Kamlin Ekambaram, Colleen Saunders, Vanessa Naidoo, Lee Wallis, Nabeela Amien, Tasleem Ras, Klaus von Pressentin, Gamuchirai Tadzimirwa, Nadia Hussey, Steve Reid, and Peter Hodgkinson. A COVID-19 field hospital in a conference centre – The Cape Town, South Africa experience. *African Journal of Primary Health Care & Family Medicine*, 2021. ISSN 2071-2928. doi:<https://doi.org/10.4102/phcfm.v13i1.3140>.
- Amy W. Baughman, Ronald E. Hirschberg, Larissa J. Lucas, Elliot D. Suarez, Deanna Stockmann, Stacy Hutton Johnson, Matthew M. Hutter, Deborah J. Murphy, Regan H. Marsh, Ryan W. Thompson, Giles W. Boland, Jeanette Ives Erickson, and Kerri Palamara. Pandemic Care Through Collaboration: Lessons From a COVID-19 Field Hospital. *Journal of the American Medical Directors Association*, 21(11):1563–1567, 2020. ISSN 1525-8610. doi:<https://doi.org/10.1016/j.jamda.2020.09.003>.
- Lyudmyla Kompaniyets, Audrey F Pennington, Alyson B Goodman, and Hannah G et al Rosenblum. Underlying Medical Conditions and Severe Illness Among 540,667 Adults Hospitalized With COVID-19, March 2020-March 2021. *Preventing Chronic Disease*, 18:E66, 2021. ISSN 1545-1151. doi:<https://doi.org/10.5888/pcd18.210123>.
- Gareth James, Daniela Witten, Trevor Hastie, and Robert Tibshirani. *An Introduction to Statistical Learning*. Springer, 01 2013. ISBN 1461471389.
- Adrian D. Haimovich, Neal G. Ravindra, Stoytcho Stoytchev, H. Patrick Young, Francis P. Wilson, David van Dijk, Wade L. Schulz, and R. Andrew Taylor. Development and Validation of the Quick COVID-19 Severity Index: A Prognostic Tool for Early Clinical Decompensation. *Annals of Emergency Medicine*, 76(4):442–453, 2020a. ISSN 0196-0644. doi:<https://doi.org/10.1016/j.annemergmed.2020.07.022>.
- Guangyao Wu, Pei Yang, Yuanliang Xie, Henry C. Woodruff, and Xiangang et al Rao. Development of a clinical decision support system for severity risk prediction and triage of covid-19 patients at hospital admission: an international multicentre study. *European Respiratory Journal*, 56(2), 2020. ISSN 0903-1936. doi:<https://doi.org/10.1183/13993003.01104-2020>.
- Dhruv Patel, Vikram Kher, Bhushan Desai, Xiaomeng Lei, Steven Cen, Neha Nanda, Ali Gholamrezanezhad, Vinay Duddalwar, Bino Varghese, and Assad Oberai. Machine learning based predictors for covid-19 disease severity. 11 2020a. doi:10.21203/rs.3.rs-108301/v1.
- Patrick Schwab, August DuMont Schütte, Benedikt Dietz, and Stefan Bauer. predcovid-19: A systematic study of clinical predictive models for coronavirus disease 2019. *CoRR*, abs/2005.08302, 2020.
- Yue Gao, Guangyao Cai, Wei Fang, Hua-Yi Li, Si-Yuan Wang, and Lingxi et al Chen. Machine learning based early warning system enables accurate mortality risk prediction for covid-19. *Nature Communications*, 11:1–10, 10 2020. doi:<https://doi.org/10.1038/s41467-020-18684-2>.
- Chuanyu Hu, Zhenqiu Liu, Yanfeng Jiang, Oumin Shi, Xin Zhang, and et al. Early prediction of mortality risk among patients with severe COVID-19, using machine learning. *International Journal of Epidemiology*, 49(6):1918–1929, 09 2020. ISSN 0300-5771. doi:<https://doi.org/10.1093/ije/dyaa171>.
- Mohammadreza Nemati, Jamal Ansary, and Nazafarin Nemati. Machine-learning approaches in covid-19 survival analysis and discharge-time likelihood prediction using clinical data. *Patterns*, 1(5):100074, 2020. ISSN 2666-3899. doi:<https://doi.org/10.1016/j.patter.2020.100074>.
- Augusto Di Castelnuovo, Marialaura Bonaccio, Simona Costanzo, and Alessandro Gialluisi et al. Common cardiovascular risk factors and in-hospital mortality in 3,894 patients with covid-19: survival analysis and machine learning-based findings from the multicentre italian corist study. *Nutrition, Metabolism and Cardiovascular Diseases*, 30(11):1899–1913, 2020. ISSN 0939-4753. doi:<https://doi.org/10.1016/j.numecd.2020.07.031>.
- Ian Goodfellow, Yoshua Bengio, and Aaron Courville. *Deep Learning*. MIT Press, 2016.

- Youssoufa Mohamadou, Aminou Halidou, and Pascal Tiam Kapen. A review of mathematical modeling, artificial intelligence and datasets used in the study, prediction and management of COVID-19. *Applied Intelligence*, 50: 3913–3925, 2020.
- Ebenezer Jangam, Aaron Antonio Dias Barreto, and Chandra Sekhara Rao Annavarapu. Automatic detection of COVID-19 from chest CT scan and chest X-Rays images using deep learning, transfer learning and stacking. *Applied Intelligence*, 52(2):2243–2259, 2022. ISSN 15737497. doi:<https://doi.org/10.1007/s10489-021-02393-4>.
- Shouliang Qi, Caiwen Xu, Chen Li, Bin Tian, Shuyue Xia, Jigang Ren, Liming Yang, Hanlin Wang, and Hui Yu. Dr-mil: deep represented multiple instance learning distinguishes covid-19 from community-acquired pneumonia in ct images. *Computer Methods and Programs in Biomedicine*, 211:106406, 2021. ISSN 0169-2607. doi:<https://doi.org/10.1016/j.cmpb.2021.106406>.
- Nathalie Lassau, S. Ammari, Emilie Chouzenoux, Hugo Gortais, Paul Herent, Matthieu Devilder, Samer Soliman, Olivier Meyrignac, Marie-Pauline Talabard, Jean-Philippe Lamarque, Remy Dubois, Nicolas Loiseau, Paul Trichelair, Etienne Bendjebbar, Gabriel Garcia, Corinne Balleyguier, Mansouria Merad, Annabelle Stoclin, Simon Jegou, and Michael Blum. Integrating deep learning ct-scan model, biological and clinical variables to predict severity of covid-19 patients. *Nature Communications*, 12:634, 01 2021. doi:<https://doi.org/10.1038/s41467-020-20657-4>.
- Asif Iqbal Khan, Junaid Latief Shah, and Mohammad Mudasar Bhat. Coronet: A deep neural network for detection and diagnosis of covid-19 from chest x-ray images. *Computer Methods and Programs in Biomedicine*, 196:105581, 2020. ISSN 0169-2607. doi:<https://doi.org/10.1016/j.cmpb.2020.105581>.
- Samson Anosh Babu P and Chandra Sekhara Rao Annavarapu. Deep learning-based improved snapshot ensemble technique for COVID-19 chest X-ray classification. *Applied Intelligence*, 51(5):3104–3120, 2021. ISSN 15737497. doi:<https://doi.org/10.1007/s10489-021-02199-4>.
- Xiaoran Li, Peilin Ge, Jocelyn Zhu, Haifang Li, James Graham, Adam Singer, Paul Richman, and Tim Duong. Deep learning prediction of likelihood of icu admission and mortality in covid-19 patients using clinical variables. *PeerJ*, 8:e10337, 11 2020. doi:<https://doi.org/10.7717/peerj.10337>.
- Yongjin Li and Jagdish Patra. Genome-wide inferring gene-phenotype relationship by walking on the heterogeneous network. *Bioinformatics (Oxford, England)*, 26:1219–24, 03 2010. doi:<https://doi.org/10.1093/bioinformatics/btq108>.
- Bo Wang, Aziz M. Mezlini, Feyyaz Demir, Marc Fiume, Zhuowen Tu, Michael Brudno, Benjamin Haibe-Kains, and Anna Goldenberg. Similarity network fusion for aggregating data types on a genomic scale. *Nature Methods*, 11: 333–337, 2014.
- Thomas N. Kipf and Max Welling. Semi-supervised classification with graph convolutional networks. *CoRR*, abs/1609.02907, 2016.
- Matthias Keicher, Hendrik Burwinkel, David Bani-Harouni, Magdalini Paschali, Tobias Czempiel, Egon Burian, Marcus R. Makowski, Rickmer Braren, Nassir Navab, and Thomas Wendler. U-gat: Multimodal graph attention network for covid-19 outcome prediction. 2021.
- Xiang Yu, Siyuan Lu, Lili Guo, Shui-Hua Wang, and Yu-Dong Zhang. Resgnet-c: A graph convolutional neural network for detection of covid-19. *Neurocomputing*, 452:592–605, 2021. ISSN 0925-2312. doi:<https://doi.org/10.1016/j.neucom.2020.07.144>.
- Elisa Ferrari, Luna Gargani, Greta Barbieri, Lorenzo Ghiadoni, Francesco Faita, and Davide Bacciu. A causal learning framework for the analysis and interpretation of covid-19 clinical data. *PLOS ONE*, 17(5):1–21, 05 2022. doi:<https://doi.org/10.1371/journal.pone.0268327>.
- Steven J. Krieg, Carolina Avendano, Evan Grantham-Brown, Aaron Lilienfeld Asbun, Jennifer J. Schnur, Marie Lynn Miranda, and Nitesh V. Chawla. Data-driven testing program improves detection of covid-19 cases and reduces community transmission. *medRxiv*, 2021. doi:<https://doi.org/10.1101/2021.07.31.21261423>.
- Hoon Ko, Heewon Chung, Wu Seong Kang, Kyung Won Kim, Youngbin Shin, Seung Ji Kang, Jae Hoon Lee, Young Jun Kim, Nan Yeol Kim, Hyunseok Jung, and Jinseok Lee. Covid-19 pneumonia diagnosis using a simple 2d deep learning framework with a single chest ct image: Model development and validation. *J Med Internet Res*, 22(6): e19569, Jun 2020. ISSN 1438-8871. doi:<https://doi.org/10.2196/19569>.
- Wentao Zhao, Wei Jiang, and Xinguo Qiu. Deep learning for covid-19 detection based on ct images. *Scientific Reports*, 11, 07 2021. doi:<https://doi.org/10.1038/s41598-021-93832-2>.
- Huimin Huang, Lanfen Lin, Yue Zhang, Yingying Xu, Jing Zheng, Xiongwei Mao, Xiaohan Qian, Zhiyi Peng, Jianying Zhou, Yen-Wei Chen, and Ruofeng Tong. Graph-bas3net: Boundary-aware semi-supervised segmentation network with bilateral graph convolution. In *Proceedings of the IEEE/CVF International Conference on Computer Vision (ICCV)*, pages 7386–7395, October 2021.

- Kai Xuan Lim, Yi-Tui Chen, Kuan-Ming Chiu, and Fang Ming Hung. Rush hour:transform a modern hotel into cloud-based virtual ward care center within 80 hours under covid-19 pandemic.far eastern memorialhospital's experience. *Journal of the Formosan Medical Association*, 2021. ISSN 0929-6646. doi:<https://doi.org/https://doi.org/10.1016/j.jfma.2021.10.023>.
- Stef van Buuren and Karin Groothuis-Oudshoorn. mice: Multivariate imputation by chained equations in r. *Journal of Statistical Software*, 45(3):1–67, 2011. doi:<https://doi.org/10.18637/jss.v045.i03>.
- Jiachao Wu, Jiang Shen, Man Xu, and Minglai Shao. A novel combined dynamic ensemble selection model for imbalanced data to detect covid-19 from complete blood count. *Computer Methods and Programs in Biomedicine*, 211:106444, 2021. ISSN 0169-2607. doi:<https://doi.org/10.1016/j.cmpb.2021.106444>.
- Yaguang Li, Rose Yu, Cyrus Shahabi, and Yan Liu. Diffusion convolutional recurrent neural network: Data-driven traffic forecasting. In *International Conference on Learning Representations (ICLR '18)*, 2018.
- Will Hamilton, Zhitao Ying, and Jure Leskovec. Inductive representation learning on large graphs. In I. Guyon, U. Von Luxburg, S. Bengio, H. Wallach, R. Fergus, S. Vishwanathan, and R. Garnett, editors, *Advances in Neural Information Processing Systems*, volume 30. Curran Associates, Inc., 2017.
- Guilherme Ferraz de Arruda, Francisco Rodrigues, and Yamir Moreno. Fundamentals of spreading processes in single and multilayer complex networks. *Physics Reports*, 756, 04 2018. doi:<https://doi.org/10.1016/j.physrep.2018.06.007>.
- Dhruv Patel, Vikram Kher, Bhushan Desai, Xiaomeng Lei, Steven Cen, Neha Nanda, Ali Gholamrezanezhad, Vinay Duddalwar, Bino Varghese, and Assad Oberai. Machine learning based predictors for covid-19 disease severity. *Scientific Reports*, 11 2020b. doi:<https://doi.org/10.21203/rs.3.rs-108301/v1>.
- Siavash Bolourani, Max Brenner, Ping Wang, Thomas Mcginn, Jamie Hirsch, Douglas Barnaby, and Theodoros Zanos. Development and validation of a machine learning prediction model of respiratory failure within 48 hours of patient admission for covid-19 (preprint). *Journal of Medical Internet Research*, 23, 09 2020. doi:<https://doi.org/10.2196/24246>.
- Hyung-Jun Kim, Deokjae Han, Jeong-Han Kim, Daehyun Kim, Beomman Ha, Woong Seog, Yeon-Kyeng Lee, Dosang Lim, Sung Ok Hong, Mi-Jin Park, and JoonNyung Heo. An Easy-to-Use Machine Learning Model to Predict the Prognosis of Patients With COVID-19: Retrospective Cohort Study. *Journal of Medical Internet Research*, 22(11): e24225, 2020. doi:<https://doi.org/10.2196/24225>.
- Reed AC Siemieniuk, Jessica J Bartoszko, Long Ge, Dena Zeraatkar, and Ariel et al Izcovich. Drug treatments for covid-19: living systematic review and network meta-analysis. *BMJ*, 370, 2020. doi:<https://doi.org/10.1136/bmj.m2980>.
- W S Lim, M M van der Eerden, R Laing, W G Boersma, N Karalus, G I Town, S A Lewis, and J T Macfarlane. Defining community acquired pneumonia severity on presentation to hospital: an international derivation and validation study. *Thorax*, 58(5):377–382, 2003. ISSN 0040-6376. doi:<https://doi.org/10.1136/thorax.58.5.377>.
- Christopher W. Seymour, Vincent X. Liu, Theodore J. Iwashyna, Frank M. Brunkhorst, Thomas D. Rea, André Scherag, Gordon Rubenfeld, Jeremy M. Kahn, Manu Shankar-Hari, Mervyn Singer, Clifford S. Deutschman, Gabriel J. Escobar, and Derek C. Angus. Assessment of Clinical Criteria for Sepsis: For the Third International Consensus Definitions for Sepsis and Septic Shock (Sepsis-3). *JAMA*, 315(8):762–774, 02 2016. ISSN 0098-7484.
- Adrian D. Haimovich, Neal G. Ravindra, Stoytcho Stoytchev, H. Patrick Young, Francis P. Wilson, David van Dijk, Wade L. Schulz, and R. Andrew Taylor. Development and validation of the quick covid-19 severity index: A prognostic tool for early clinical decompensation. *Annals of Emergency Medicine*, 76(4):442–453, 2020b. ISSN 0196-0644. doi:<https://doi.org/10.1016/j.annemergmed.2020.07.022>.
- Lorenzo Pellis, Francesca Scarabel, Helena B. Stage, Christopher E. Overton, Lauren H. K. Chappell, Elizabeth Fearon, Emma Bennett, Katrina A. Lythgoe, Thomas A. House, Ian Hall, and null null. Challenges in control of covid-19: short doubling time and long delay to effect of interventions. *Philosophical Transactions of the Royal Society B: Biological Sciences*, 376(1829):20200264, 2021. doi:<https://doi.org/10.1098/rstb.2020.0264>.
- Candice Downey, Rebecca Randell, Julia Brown, and David G Jayne. Continuous versus intermittent vital signs monitoring using a wearable, wireless patch in patients admitted to surgical wards: Pilot cluster randomized controlled trial. *J Med Internet Res*, 20(12):e10802, Dec 2018.
- Karen Larimer, Stephan Wegerich, Joel Splan, David Chestek, Heather Prendergast, and Terry Vanden Hoek. Personalized analytics and a wearable biosensor platform for early detection of covid-19 decompensation (decode): Protocol for the development of the covid-19 decompensation index. *JMIR Res Protoc*, 10(5):e27271, May 2021.